

Heterogeneous & Homogeneous & Bio- & Nano-

CHEM**CAT**CHEM

CATALYSIS

Accepted Article

Title: Efficient and Reusable Metal–Organic Framework Catalyst for Carboxylative Cyclization of Propargylamines with Carbon Dioxide

Authors: Dan Zhao, Xiao-Hui Liu, Chendan Zhu, Yan-Shang Kang, Peng Wang, Zhuangzhi Shi, Yi Lu, and Wei-Yin Sun

This manuscript has been accepted after peer review and appears as an Accepted Article online prior to editing, proofing, and formal publication of the final Version of Record (VoR). This work is currently citable by using the Digital Object Identifier (DOI) given below. The VoR will be published online in Early View as soon as possible and may be different to this Accepted Article as a result of editing. Readers should obtain the VoR from the journal website shown below when it is published to ensure accuracy of information. The authors are responsible for the content of this Accepted Article.

To be cited as: *ChemCatChem* 10.1002/cctc.201701190

Link to VoR: <http://dx.doi.org/10.1002/cctc.201701190>

Efficient and Reusable Metal–Organic Framework Catalyst for Carboxylative Cyclization of Propargylamines with Carbon Dioxide

Dan Zhao, Xiao-Hui Liu, Chendan Zhu, Yan-Shang Kang, Peng Wang, Zhuangzhi Shi, Yi Lu,* and Wei-Yin Sun*^[a]

Abstract: Carbon dioxide (CO₂) capture and transformation are important for continuously increasing concentration of atmospheric CO₂. To effectively capture CO₂ and further fix it into valuable chemical products, functionalized dynamic metal–organic frameworks (MOFs) have been utilized not only because of their inherent cavity for accommodating CO₂ but also due to their reversible structural transformation responsible for external stimuli for regulating the reaction. Herein, we report a dynamic and functional MOF [Cd₃(L)₂(BDC)₃]₂·16DMF (**MOF-1a**) (DMF = *N,N*-dimethylformamide) achieved by reaction of amino tripodal imidazole ligand *N*¹-(4-(1H-imidazol-1-yl)benzyl)-*N*¹-(2-aminoethyl)ethane-1,2-diamine (L) and 1,4-benzenedicarboxylic acid (H₂BDC) with cadmium salt. **MOF-1a** not only shows unprecedented high catalytic activity [initial turnover number (TON) up to 9300] and broad substrate scope for the carboxylative cyclization of propargylamines with CO₂, but also can be switched on and off upon reversible structural transformation due to its dynamic 5-fold interpenetrating structure. Further studies demonstrate that **MOF-1a** shows selective catalytic property depending on the size of substrates, like an imitation of sophisticated biological system.

Introduction

Catalytic fixing carbon dioxide (CO₂), a greenhouse gas and ubiquitous C₁ source, with amines into value-added urea derivatives has received considerable attention due to its tremendous potential economic and environmental impacts.^[1] Urea derivatives are useful chemical intermediates in synthesis of pharmaceuticals, agricultural chemicals and dyes.^[2] The synthesis of urethane derivatives through coupling reaction between CO₂ with propargylamines has been developed recently.^[3] Homogeneous catalysts such as organic bases and organometallic catalysts show high catalytic efficiency with a

wide range of substrates.^[4] Comparing with the homogeneous catalysts, metal–organic frameworks (MOFs), as a neoteric heterogeneous catalysts, provide simple workup procedure with simple filtration after the catalytic reaction, and the filtrated MOFs can be reused in the next catalytic cycle due to their robust frameworks.^[5] As the ultimate goal of catalytic research, the ideal catalysts should be efficient, recyclable, environmentally benign, good selectivity and simple workup procedure.

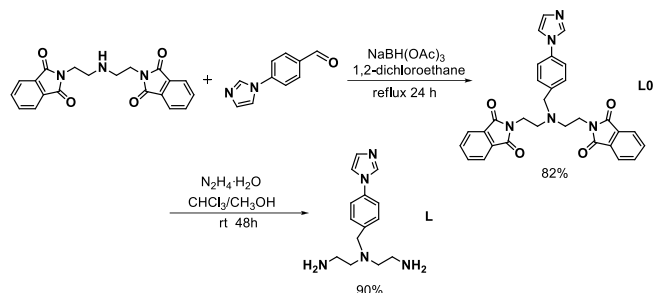
Inspired by natural enzymatic processes, chemists have attempted to emulate catalytic natural enzyme in reactions by developing efficient catalysts responsible for external stimuli to regulate the reaction rates and selectivity.^[6] Functionalized flexible MOFs are suitable platform for the development of artificial switchable catalysts because of their inherent cavities, dynamic behaviours, and the modifiable functional groups located inside the framework channels.^[7] Over the past years, an increasing number of MOFs have been discovered, exhibiting a diverse range of conformational effects, such as breathing effects and swelling.^[8] Additionally, different from other catalytic materials, the dynamic behaviours of the functionalized flexible MOFs in response to the guest molecules can induce conformational changes, which lead to selectivity of substrates as an imitation of sophisticated biological system.^[8a] In addition, much effort has been devoted to build functionalized flexible MOFs and a great deal of reports has proved that selection of metal ions is important for the construction of functionalized flexible MOFs.^[9] Compared with other transition metal ions, the soft d¹⁰ Cd(II) ion is attractive due to its diverse coordination patterns and strong coordination ability which can improve intrinsic characteristic of MOFs and the Lewis acidity of Cd(II) can enhance the catalytic activity of MOFs.^[10]

Since organic bases, such as 1,5,7-triazabicyclo[4.4.0]dec-5-ene (TBD), 1,8-diazabicyclo[5.4.0]undec-7-ene (DBU), 4-(dimethylamino)pyridine (DMAP) have been demonstrated as excellent CO₂ activators in CO₂ scrubbing to enhance the CO₂ coupling catalytic efficiency,^[11] we envision that MOFs with organic amine ligands can realize the chemical transformation of CO₂ with propargylamines to give urethane derivatives. In this work, we designed and prepared a new amino tripodal imidazole ligand *N*¹-(4-(1H-imidazol-1-yl)benzyl)-*N*¹-(2-aminoethyl)ethane-1,2-diamine (L) (Scheme 1) which was used to react with Cd(II), and finally obtained a flexible and switchable three-dimensional (3D) **MOF-1a** decorated with NH₂-groups, which can realize the cyclization reaction between CO₂ and alkynyl amines with high turnover number (TON) to construct five-membered urethane ring structures. More importantly, crystallographic analysis

[a] D. Zhao, X.H. Liu, C. Zhu, Y. S. Kang, Dr. P. Wang, Prof. Dr. Z. Shi, Prof. Dr. Y. Lu, Prof. Dr. W. Y. Sun
State Key Laboratory of Coordination Chemistry
Coordination Chemistry Institute
School of Chemistry and Chemical Engineering
Nanjing National Laboratory of Microstructure
Collaborative Innovation Center of Advanced Microstructures
Nanjing University, Nanjing 210023 (China)
Fax: (+) 86 25 89682309
E-mail: luyi@nju.edu.cn; sunwy@nju.edu.cn

Supporting information for this article can be found under:
<https://doi.org/10.1002/cctc>.

revealed that **MOF-1a** has a flexible 5-fold interpenetrating structure, and the spatial alignment of a linker is changed by turning around a rotational axis in response to the removal and rebinding of guest molecules. The unique dynamic 5-fold interpenetrating structure of **MOF-1a** can be switched on and off upon reversible structural transformation. Furthermore, **MOF-1a** shows selective heterogeneous catalytic property depending on the size of substrates.



Scheme 1. Synthetic procedure for preparation of ligand L.

Results and Discussion

Reactions of amino tripodal imidazole ligand L, $\text{Cd}(\text{ClO}_4)_2 \cdot 6\text{H}_2\text{O}$, 1,4-benzenedicarboxylic acid (H_2BDC) in mixed solvent of *N,N*-dimethylformamide (DMF) and methanol at 90 °C for 3 days yielded crystals **MOF-1a**. Complete deprotonation of H_2BDC to give BDC^{2-} in **MOF-1a** was confirmed by IR spectral data since no vibration bands were observed between 1680 - 1760 cm^{-1} (Figure S1 in the Supporting Information).

Crystal Structure Description

The results of crystallographic analysis revealed that **MOF-1a** crystallizes in monoclinic space group $C2/c$, and the coordination environment around $\text{Cd}(\text{II})$ is shown in Figure S2 in the Supporting Information. $\text{Cd}1$ is coordinated by three nitrogen atoms (N1, N2 and N3) from one L ligand and three carboxylate oxygen ones (O1, O2 and O3) from two different BDC^{2-} to give a distorted octahedral coordination geometry, while $\text{Cd}2$ adopts a coordination donor set of N_2O_4 , which is comprised by two imidazole nitrogen atoms (N5B and N5D) from two different L, and four carboxylate oxygen ones (O5, O6, O5A and O6A) from two different BDC^{2-} ligands.

The framework of **MOF-1a** is constructed from the $\text{Cd}(\text{II})$ as three- and four-connected nodes, L and BDC^{2-} as two-connected linkers. The coordination modes of ligands L and BDC^{2-} are illustrated in Figure S3 in the Supporting Information. This arrangement produces a large $9.918 \times 8.013 \text{ \AA}^2$ rectangle subunit composed of four $\text{Cd}(\text{II})$ linked together by two L and two BDC^{2-} (Figure S4 in the Supporting Information). The adjacent rectangle subunits connect with each other by $\text{Cd}2$ to generate an infinite one-dimensional (1D) chain as shown in Figure 1a. The 1D chain expands in three directions by BDC^{2-} to form a 3D framework as shown in Figure 1b. To better understand the

nature of this intricate architecture, topological analysis was carried out.^[12] $\text{Cd}1$ and $\text{Cd}2$ can be considered as three- and four-connected nodes respectively, and accordingly a (3,4)-connected 2-nodal 3D net with a point symbol of $\{4 \cdot 10^2\}_2\{4^2 \cdot 10^4\}$ is generated (Figure 1c). Interestingly, five sets of such 3D nets mutually interpenetrate each other to result a 5-fold interpenetrating structure (Figure 1d). This interpenetrating behaviour could be well recognized as a self-complementary of crystal stability.

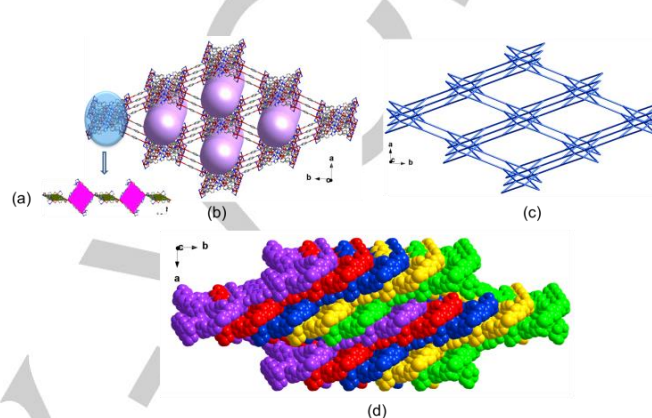


Figure 1. (a) An infinite 1D chain structure composed of rectangle subunits. (b) 3D framework of **MOF-1a**. (c) Topological presentation of the 3D framework of **MOF-1a**. (d) 5-Fold interpenetrating structure of **MOF-1a** (each colour represents a 3D framework).

In addition, along *b* axis, the 5-fold interpenetrating 3D framework has two types of channels (**A** and **B**) available for guest molecules accommodation and exchange (Figure 2a). The solvent accessible volume is 4120.8 \AA^3 out of the 8375.0 \AA^3 unit cell volume after removal of DMF molecules (49.2% of the total crystal volume), calculated by PLATON.^[13] Both the larger channel **A** with dimension of $10.5 \times 6.3 \text{ \AA}^2$ and the smaller one **B** with dimension of $5.1 \times 6.3 \text{ \AA}^2$ are occupied by DMF molecules. Consequently, the NH_2 -groups, highly ordered on the surfaces of the channels, can interact with guest molecules (Figure 2b).

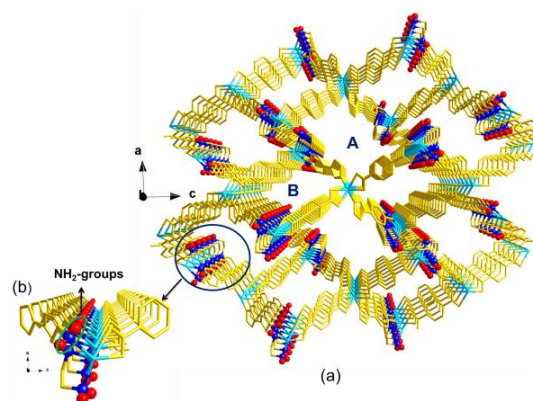


Figure 2. (a) Channels in **MOF-1a**. DMF molecules are omitted for clarity. (b) View of the part ordered NH_2 -groups on the channel surface (red balls: H).

Dynamic Structure

It can be seen from the crystal structure analysis that **MOF-1a** includes 16 DMF guest molecules per formula unit, which is in accordance with the TG result (Figure S5 in the Supporting Information). **MOF-1a** was immersed in acetone for 2 days to remove the non-volatile solvent molecules. After drying under vacuum for 24 h at 40 °C, colorless powder **MOF-1b** was obtained. The TG curve of **MOF-1b** suggests that the guest molecules in **MOF-1a** are completely removed (Figure S5 in the Supporting Information).

Table 1. Unit cell parameters of **MOF-1a** and **MOF-1b**.

	MOF-1a	MOF-1b
Empirical formula	C ₁₅₂ H ₂₂₀ Cd ₆ N ₃₆ O ₄₀	C ₁₀₄ H ₁₀₈ Cd ₆ N ₂₀ O ₂₄
Crystal system	Monoclinic	Monoclinic
Space group	C2/c	C2/c
<i>a</i> /Å	27.915(4)	26.183
<i>b</i> /Å	10.6683(15)	11.360
<i>c</i> /Å	29.421(4)	19.733
β /°	91.081(2)	98.398
<i>R</i> _p	–	10.186

Interestingly, the different PXRD patterns of **MOF-1a** and **MOF-1b** imply that they have different structures, even **MOF-1b** has good crystallinity after the desolvation (Figure S6 in the Supporting Information). From the PXRD results, it was suggested that the sub-network of **MOF-1a** might be displaced in response to the removal and rebinding of the solvent molecules, owning the so-called ‘dynamic structure’. This sub-network displacement often occurs in the interpenetrating structures, which have individual concatenated frameworks interacting with each other by rather weak forces such as van der Waals and/or hydrogen bonding interactions, and thus they can drift, relocate, or shift to some extent in regard to each other.^[8a] The unit cell parameters of the desolvated sample **MOF-1b** is obtained by analysis and fitting the PXRD pattern using *TOPAS v4.2 software* (Table 1 and Figure S7 in the Supporting Information).^[14] Comparing the cell parameters of **MOF-1a** and **MOF-1b**, *a*-axis and *b*-axis are similar, while the *c*-axis is reduced from 29.421 to 19.733 Å, indicating that a large sub-network displacement occurred. In addition, the guest molecule responsive behavior of **MOF-1a** was also examined by using single-crystal X-ray diffraction under N₂ flow. As a result, a thermal-induced dynamic behavior was observed for the crystal, which exhibits a phase transition around 330 K (Figure 3 and Table S3 in the Supporting Information). In this narrow temperature range, the unit-cell parameters of *a*-axis and *b*-axis are nearly unchanged after heating, while the *c*-axis is reduced

to 19.8199(8) at 333 K, agreeing well with the result from the PXRD pattern fitting. In order to further validate the dynamic structure of **MOF-1a**, reversible experiment was carried out. The colorless powder **MOF-1b** was soaked in DMF/CH₃OH. After heated at 90 °C for 72 h, the pale yellow powder was obtained. The PXRD pattern evidences the recovery of **MOF-1a** (Figure S6 in the Supporting Information). In general, the experimental results show that **MOF-1a** has a unique dynamic 5-fold interpenetrating structure, which can be switched on and off upon reversible structural transformation by elimination and rebinding of guest molecules.

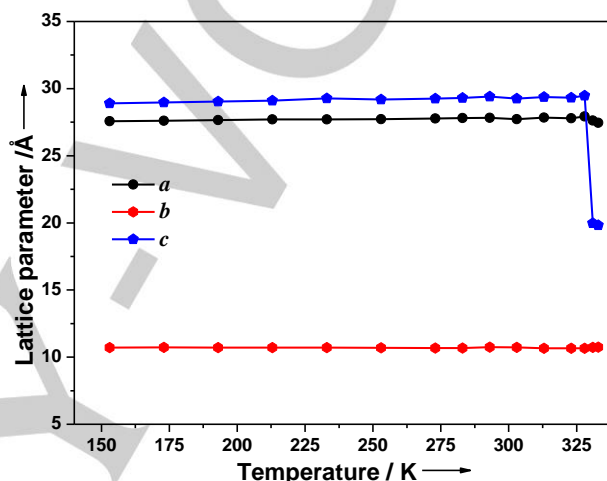


Figure 3. Temperature dependent unit-cell parameters of **MOF-1a**.

Sorption Property of **MOF-1b**

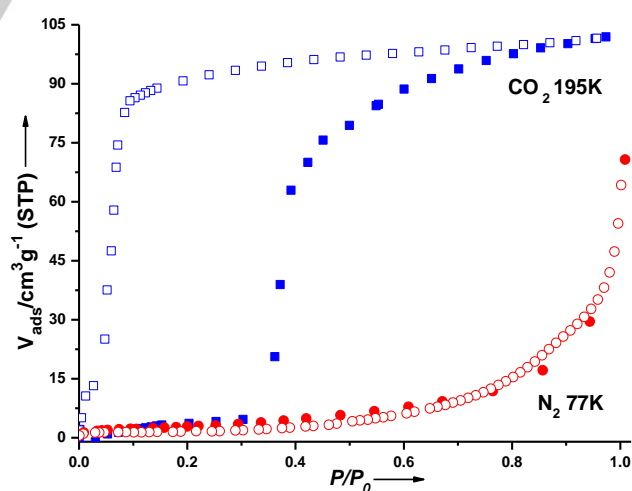


Figure 4. Gas adsorption isotherms of **MOF-1b** for N₂ (77 K) and CO₂ (195 K): filled shape, adsorption; open shape, desorption.

With the concept that the softness and flexibility of MOFs with catenation and inter-digitation is possible to induce guest recognition and selection, we performed N₂ (77 K) and CO₂ (195 K) adsorption measurements of **MOF-1b**. As shown in Figure 4, almost no sorption of N₂ at 77 K was detected, particularly at low pressure, implying non-porous structure of **MOF-1b**. In contrast, **MOF-1b** shows a rather interesting CO₂ sorption isotherm at 195 K. From a P/P_0 pressure of ca. 0.3, an abrupt increase of the adsorption of CO₂ was found and then finally attains saturation with the maximum value of 101.93 cm³ g⁻¹ at 195 K under P/P_0 pressure of 1.0. In addition, the desorption isotherm of CO₂ exhibits steps at the corresponding inflection points of the adsorption isotherm, but does not trace the adsorption profile and decreases slightly until a sudden drop at $P/P_0 = 0.1$ with a large-range hysteresis loop. Namely, the remarkable hysteresis loop between the adsorption and desorption isotherms indicates that the adsorbed CO₂ molecules are not immediately released when the external pressure decreased, confirming that CO₂ molecules are trapped within the framework. Furthermore, adsorptions of CO₂ at 273 and 298 K were measured. As shown in Figure S8 in the Supporting Information, adsorption isotherms of CO₂ at 273 and 298 K also exhibit hysteresis with CO₂ uptake of 9.34 cm³ g⁻¹ at 273 K and 4.15 cm³ g⁻¹ at 298 K at ambient pressure. From these results, we conclude that the NH₂-groups inside the channel surfaces function effectively, raising the attractive interactions of MOFs with CO₂ molecules. Such characteristic sorption isotherm is a typical sign for a non-porous to porous structural transformation, which occurs at a certain gate-opening pressure.^[15] The structural transformation of the dynamic frameworks can be stimulated by the interaction between the guest molecules and the host framework.

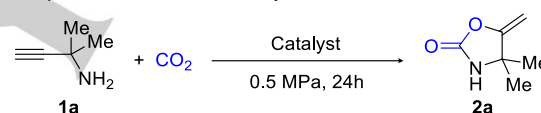
Carboxylative Cyclization of CO₂ with Propargylamines

The dynamic behaviour of the flexible MOFs allows the cavity environment to be tuned by external stimuli, which in turn influence the catalytic activity of the heterogeneous catalysts. However, flexible MOFs for switchable catalysis have not been well explored, probably because of the close-conformation of flexible MOFs which can be opened up by solvent molecules under catalytic conditions.^[8a] Both **MOF-1a** and **MOF-1b** can maintain its inherent structure in most organic solvents, such as acetonitrile, acetone and methanol at room temperature. Moreover, the structural transformation of **MOF-1a** and **MOF-1b** happens only in DMF/CH₃OH after heated at 90 °C for 72 h. Overall, these observations suggest that **MOF-1a** and **MOF-1b** can be considered as “rigid” under common catalytic reaction conditions. Considering the dynamic and functionalized feature of **MOF-1a**, the carboxylative cyclization of CO₂ with propargylamines catalyzed by **MOF-1a** has been performed.

We selected 1,1-dimethylpropargylamine (**1a**) as the initial substrate for the cyclization reaction (Table 2). A brief solvent screen of this reaction indicated that acetonitrile was the ideal solvent for achieving high yields. An initial investigation was carried out with 0.4 mol% catalyst loading based on NH₂-groups of **MOF-1a**, as well as other catalysts, at 60 °C under 0.5 MPa in acetonitrile for 24 h. Catalyst **MOF-1a** gave the product 4,4-

dimethyl-5-methyleneoxazolidin-2-one (**2a**) in 92% NMR yield (Table 2, entry 1). The basic ligand L presented 86% NMR yield of **2a**, while the acid ligands failed to give the desired product, showing that the organic amine ligand had good catalytic activity for this reaction (Table 2, entries 2–4). The influence of DMF molecule on the reaction was explored as well due to a large number of DMF molecules in the skeleton of **MOF-1a**, however, no desired product was obtained (Table 2, entry 5). Perchlorate salt Cd(ClO₄)₂·6H₂O was also tested as catalyst, and only 22% NMR yield of **2a** could be obtained probably due to in situ formation of a less active species Cd acetylide (Table 2, entry 6). To recap briefly, the basic ligand L and **MOF-1a** showed superior catalytic activity than the other catalysts in the conversion of **1a** to **2a** under the same conditions. Compared with the basic ligand L, **MOF-1a** shows heterogeneous catalytic property and the reaction of **1a** proceeded smoothly to give corresponding **2a** in good yield after 24 h under 0.5 MPa, even if the catalyst loading reduced to 0.01 mol%, indicating that the **MOF-1a** was stable enough for the carboxylation to give TON up to 8500 (Table 3, entry 1). However, when the reaction was carried out under 0.1 MPa, the yield of **2a** was less than 40%, no matter at room temperature or higher temperature (Table 3, entry 1).

Table 2. Optimization of reaction catalysts and conditions.^[a]



Entry	Catalyst (mol%)	Solvent (3 ml)	NMR yield (%) ^[b]
1	MOF-1a (NH ₂ : 0.4)	DMSO MeCN	52 92
2	L (NH ₂ : 0.2)	MeCN	86
3	Disodium Terephthalate (0.3)	MeCN	ND
4	H ₂ BDC (0.3)	MeCN	ND
5	DMF (0.3)	MeCN	ND
6	Cd(ClO ₄) ₂ ·6H ₂ O (0.3)	MeCN	22

[a] Reaction conditions: **1a** (1 mmol). [b] NMR yield was determined by ¹H NMR analysis of the crude reaction mixture using hexamethylcyclotrisiloxane as the internal standard.

With the optimized condition in hand, we set out to investigate the scope of substrates. First, we focused on terminal propargylamines for their small size and high activity (Table 3). Notably, the *N*-methylpropargylamine (**1b**) gave the corresponding oxazolidinone (**2b**) in >99% yield with a catalyst loading of 0.4 mol% (Table 3, entry 2). Furthermore, a higher TON (9300) than the previous reported ones can be achieved when the catalyst loading was 0.01 mol% (Table 3, entry 2 and

Table S4 in the Supporting Information).^[16] Terminal propargylamine **1c**, **1d** and **1e** gave the corresponding urea derivatives **2c**, **2d** and **2e** in good yields, indicating high versatility of this catalytic system (Table 3, entries 3–5). The

substrate **1f** gave 32% yield because of the steric effects exerted by the cyclohexyl (Table 3, entry 6). In general, the combined results and the highest TON indicated that **MOF-1a** owned good catalytic activity for terminal propargylamines.

Table 3. Cyclization reaction of CO₂ with terminal propargylamines.^[a]

Entry	Substrate	Product	CO ₂ (MPa)	Temperature (°C)	Catalyst loading (NH ₂ : mol%)	Yield (%)	TON ^[d]
1			0.1	I: 25 II: 60	0.8 0.8	<5% ^[b] 30 ^[b]	
			0.5	60	I: 0.8 II: 0.4 III: 0.1 IV: 0.04 V: 0.01	98 ^[b] 95 ^[b] 95 ^[b] 93 ^[b] 85 ^[c]	8500
2			0.5	60	I: 0.4 II: 0.01	>99 ^[b] 93 ^[c]	9300
3			0.5	60	0.4	89 ^[c]	
4			0.5	60	0.4	91 ^[c]	
5			0.5	60	0.4	62 ^[c]	
6			0.5	60	0.4	32 ^[c]	

[a] Reaction conditions: substrates (1 mmol), CH₃CN (3 ml). [b] NMR yield was determined by ¹H NMR analysis of the crude reaction mixture using hexamethylcyclotrisiloxane as the internal standard. [c] Isolated yield. [d] TON = (moles of product)/(moles of catalyst).

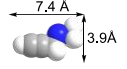
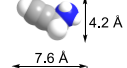
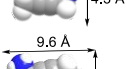
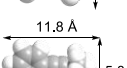
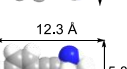
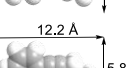
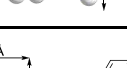
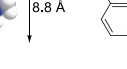
Substrate Selectivity in Cyclization Reaction

High activity of **MOF-1a** for cyclization reaction of CO₂ and terminal propargylamines illustrates that smaller substrates with the width less than 4.3 Å can enter the channels and finally finish catalytic reactions (Table 4, **1b** and **1c**). To confirm the

selective accommodation and activation of reactants by **MOF-1a**, substrates with different size were selected to identify the selectivity of **MOF-1a**. Substrates with terminal methyl and ethyl units, but-2-yn-1-amine (**1g**) and pent-2-yn-1-amine (**1h**) gave the products **2g** and **2h** in good yields. The width of the substrates, substituted by phenyl (**1i**, **1j** and **1k**), was further

increased, and the corresponding products (**2i**, **2j** and **2k**) could also be detected. The product **2k** was in good yield probably because of the electron-donating group (methyl group) of the secondary amine. However, products **2i** and **2j** were obtained in poor yields, especially for **2j**, probably because of the large steric effect from the two methyl groups and the cyclohexyl group, respectively. Further increase of the substrates size to 8.8 and 8.9 Å (**1l** and **1m**) gave no desired products. The results are in accordance to the fact that the width of channels in **MOF-1a** is about 6.9 Å for channel **A** and 5.6 Å for channel **B**, indicating that this substrate-selective reaction occurs in the channels rather than the surface of **MOF-1a**.

Table 4. Substrate selectivity in cyclization reaction.^[a]

			>99%
			89%
			81%
			74%
			31%
			<5%
			82%
			
			

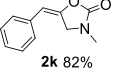
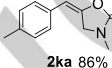
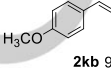
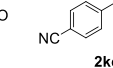
[a] Reaction conditions: **MOF-1a** (NH₂: 0.4 mol%), substrates (1 mmol), CH₃CN (3 ml) under CO₂ (0.5 MPa) at 60 °C for 24 h. The yields were calculated using the isolated product.

To investigate the generality of catalyst **MOF-1a**, a range of different substituted phenylethyneamines have been tested under the optimized reaction conditions (Table 5). Unsubstituted phenylethyneamine provided desired product (**2k**) with high yield of 82%. For *para*-substituted substrates, those bearing electron-donating groups gave the desired products (**2ka** and **2kb**) in excellent yields, while the one with electron-withdrawing group gave the desired product (**2kc**) with a much lower yield of 38% because of the electronic effect exerted by the nitrile group.

Because of the reversible structural transformation of **MOF-1a** and **MOF-1b**, the selective accommodation and activation of reactants by **MOF-1b** were also investigated. Unlike **MOF-1a**,

MOF-1b catalyzed the reactions of terminal propargylamines with the width less than 4.2 Å under CO₂ (0.5 MPa) at 60 °C (Table S5 in the Supporting Information). Such catalytic selectivity results have proved the existence of porosity of **MOF-1b** under high pressure (0.5 MPa), which is consistent with adsorption analysis for **MOF-1b**.^[17] The experiment results perfectly illustrate that **MOF-1a** is a flexible and switchable catalyst for the catalytic selectivity over substrates, like an imitation of sophisticated biological systems.

Table 5. Scope of the phenylethyneamine substrates.^[a]

			
2k 82%	2ka 86%	2kb 90%	2kc 38%

[a] Reaction conditions: **MOF-1a** (NH₂: 0.4 mol%), substrates (1 mmol), CH₃CN (3 ml) under CO₂ (0.5 MPa) at 60 °C for 24 h. The yields were calculated using the isolated product.

Proposed Catalytic Pathway

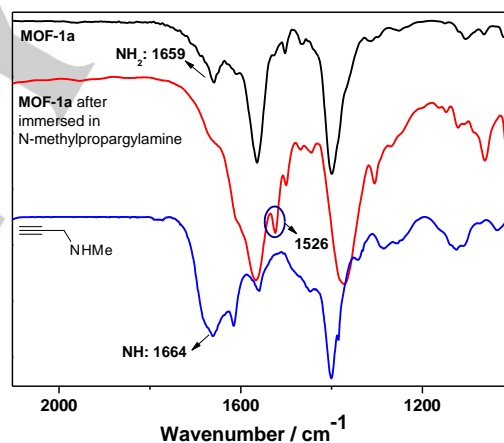


Figure 5. Partial IR spectra of **MOF-1a** (black), **MOF-1a** impregnated with *N*-methylpropargylamine (red), and *N*-methylpropargylamine (blue).

The high activity of **MOF-1a** for cyclization reaction of CO₂ and propargylamines has prompted us to investigate the proposed reaction pathway. In order to clarify the catalytic active sites, the infrared spectra of **MOF-1a**, **MOF-1a** after immersed in *N*-methylpropargylamine, and *N*-methylpropargylamine were measured (Figure S1a in the Supporting Information). To further study the ascription of infrared characteristic peaks, the IR vibrating peaks of *N*-methylpropargylamine were calculated using Gaussian AM1 (Table S6 and Figure S1b in the Supporting Information). As a result, the peaks at 1664 cm⁻¹ in the spectrum of *N*-methylpropargylamine and 1659 cm⁻¹ in the spectrum of **MOF-1a** are corresponding to the characteristic peaks of -NH and -NH₂ bending vibration, respectively. Moreover,

after immersed in *N*-methylpropargylamine for 6 h, the bending vibration peak of $-\text{NH}_2$ (1659 cm^{-1}) in **MOF-1a** has disappeared, meanwhile, a new peak exhibits at 1526 cm^{-1} which is correspond to the characteristic infrared peak of amine salt (Figure 5). Therefore, we propose that the basicity of the NH_2 -groups in catalyst **MOF-1a** is important to the catalytic reaction. The mechanism is proposed as follows: CO_2 was activated by propargylamines; the NH_2 -groups in **MOF-1a** promoted an efficient ring closure to the oxazolidinones derivative, which was rather stable under the reaction conditions (Figure 6).^[11a,11b]

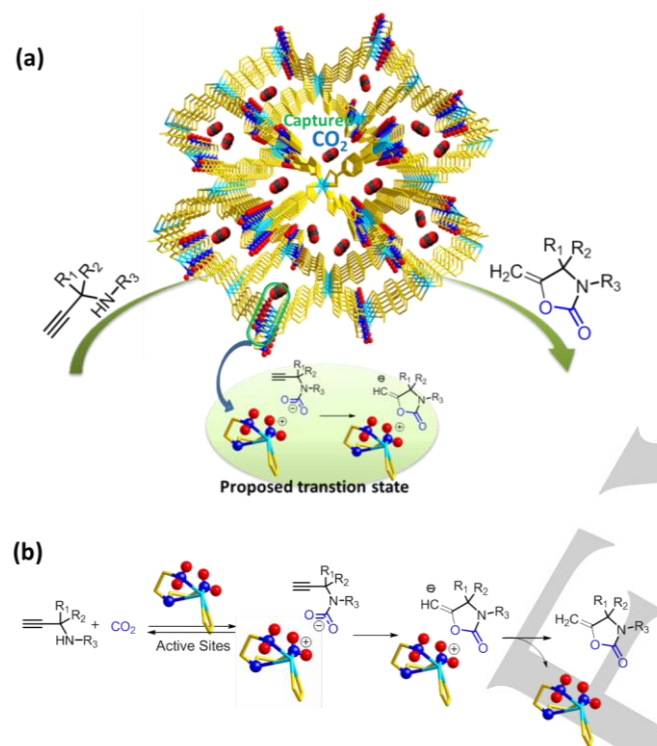


Figure 6. (a) Proposed formation pathway for methyleneoxazolidinones. (b) Details of the proposed formation pathway.

Recycling Stability of MOF-1a

Reusability is the key issue for practical application of the heterogeneous catalysts, which makes them more beneficial over the homogeneous counterparts.^[18] Ideal heterogeneous catalysts should exhibit high catalytic activity and selectivity, and maintain their catalytic activities over several cycles of the reaction. We found that **MOF-1a** could be reused up to 4 times without significant changes under CO_2 pressure of 0.5 MPa and elevated temperature ($60\text{ }^\circ\text{C}$) after 24 h. The substrate, 1,1-dimethylpropargylamine (**1a**) could proceed smoothly to give corresponding **2a** with a catalyst loading of 0.4 mol% (Figure 7a). After the reaction, **MOF-1a** from the reaction isolated by simple filtration was used for the successive runs. The reaction yield of **2a** was not significantly affected in additional cycles (Figure 7b), although the loss of small amounts of the catalyst is unavoidable

(Table S7 in the Supporting Information). The amount of $\text{Cd}(\text{II})$ leached to the reaction mixture after the catalyst isolation is 6.78 ppm determined by ICP-MS measurements, implying loss of about 3% of catalyst **MOF-1a** in the catalytic reaction. Furthermore, XRD patterns and IR data of the reused crystals confirm the stability of **MOF-1a** (Figure 7c and Figure S9 in the Supporting Information).

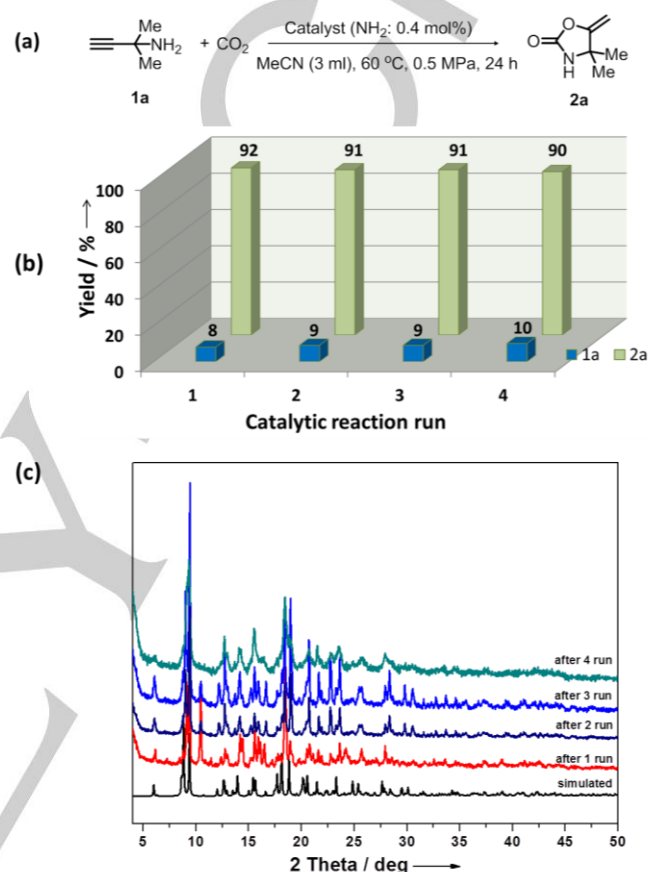


Figure 7. (a) Cyclization reaction of CO_2 and 1,1-dimethylpropargylamine. (b) Catalytic activity and the recycling of **MOF-1a**. (c) PXRD patterns of **MOF-1a** in recycling stability experiments.

Conclusions

In conclusion, this work describes the construction of a flexible and switchable 3D **MOF-1a** that is decorated with NH_2 -groups realizing the capture and transformation of CO_2 . Remarkably, **MOF-1a** shows unprecedented high activity for the cyclization reaction of CO_2 with propargylamines, and the TON value can be up to 9300. To the best of our knowledge, the TON is higher than the previously reported results for a catalytic system in the context of 2-oxazolidinones formation. More importantly, the unique dynamic 5-fold interpenetrating structure of **MOF-1a** can be switched on and off upon reversible structural transformation, and finally demonstrates its selective heterogeneous catalytic property, which depends on the size of substrates, like an

imitation of sophisticated biological system. In addition, the promising structure features of catalyst **MOF-1a** make it exhibit excellent catalytic property including substrate scope versatility, wide functional group tolerance, highly product yield and catalyst reusability.

Experimental Section

Materials and Instrumentation

Compounds of 4-(1H-imidazol-1-yl)benzaldehyde and bis(2-phthalimidoethyl)amine were prepared according to the previously reported procedure.^[19] H₂BDC and Cd(ClO₄)₂·6H₂O were obtained from Aladdin Industrial Corporation. All catalytic reactions were carried out under carbon dioxide atmosphere unless otherwise noted. Reactions were monitored by thin-layer chromatography (TLC) on silica gel plates (GF254), and the analytical TLC was performed on pre-coated, glass-backed silica gel plates. ¹H-, ¹³C-NMR spectra were recorded on Bruker-DRX (400 MHz) instruments at room temperature. Abbreviations for signal couplings are: s, singlet; d, doublet; t, triplet; m, multiplet. High-resolution mass spectra were obtained on AGILENT 6540QTOF for Mass Spectrometry, Nanjing University. Elemental analyses for C, H, and N were performed on Elemental Vario MICRO at the analysis center of Nanjing University. FT-IR spectra were measured in the range of 400-4000 cm⁻¹ on a Bruker Vector 22 FT-IR spectrophotometer using KBr pellets. Thermogravimetric analyses (TGA) were performed on a Mettler-Toledo (TGA/DSC1) thermal analyzer under nitrogen with a heating rate of 10 °C min⁻¹. Powder X-ray diffraction (PXRD) data were achieved on a Bruker D8 Advance X-ray diffractometer with Cu Kα (λ = 1.5418 Å) radiation. The adsorption isotherms of nitrogen and carbon dioxide were obtained on a Belsorp-max volumetric gas sorption instrument. Inductively coupled plasma mass spectrometer (ICP-MS) measurements were carried out on Optima 5300DV.

Single-Crystal X-ray Structure Determination

Diffraction data for **MOF-1a** were collected on a Bruker Smart Apex CCD area detector diffractometer with graphite-monochromated Mo-Kα radiation (λ = 0.71073 Å) at 293(2) K using the ω-scan technique. The data were integrated by using SAINT program, which was also used for intensity corrections for Lorentz and polarization effects. Semi-empirical absorption corrections were applied using the SADABS program and the structure was solved by direct methods and refined on F² by the full-matrix least-squares methods using the SHELXTL package.^[20] The detailed crystal data and selected bond lengths and angles for **MOF-1a** are given in Table S1 and Table S2 in the Supporting Information. CCDC 1544531 (**MOF-1a**) contain the supplementary crystallographic data for this paper. These data are provided free of charge by The Cambridge Crystallographic Data Centre.

Synthesis of Ligand (L)

To a 1,2-dichloroethane (150 ml) solution of bis(2-phthalimidoethyl)amine (10.0 g, 28 mmol) in a 500 ml round-bottom flask, 4-(1H-imidazol-1-yl)benzaldehyde (4.8 g, 28 mmol) was added in one portion at room temperature. Subsequently, NaBH(OAc)₃ (8.6 g, 39 mmol) was added, and the mixture was heated to reflux for 24 h. After cooling to room temperature, the reaction mixture was diluted with H₂O (100 ml), extracted with dichloromethane (2 x 100 ml). The combined organics were washed with brine, dried over MgSO₄, and then concentrated to 10 ml. CH₃OH (150 ml) was then added to give colorless precipitates L0 (11.9 g, 82% yield). ¹H NMR (400 MHz, CDCl₃): δ 7.64-7.74 (m, 9 H),

7.13-7.20 (m, 4 H), 6.84-6.91 (m, 2 H), 3.76 (t, J = 6.0 Hz, 4 H), 3.69 (s, 2 H), 2.82 (t, J = 6.0 Hz, 4 H). To a CHCl₃/EtOH (300 ml, v/v, 1:5) solution of L0 (5.2 g, 10 mmol), H₂NNH₂·H₂O (0.5 g, 10.0 mmol) was added by portions at room temperature. The reaction mixture was stirred at room temperature for 24 h, and then filtered off. The yellow oil L (2.3 g, 90% yield) was obtained by evaporation of the filtrate. ¹H NMR (400 MHz, CDCl₃): δ 7.75 (d, J = 1.1 Hz, 1 H), 7.32-7.38 (m, 2 H), 7.23-7.28 (m, 2 H), 7.19 (t, J = 1.4 Hz, 1 H), 7.11 (t, J = 1.2 Hz, 1 H), 3.57 (s, 2 H), 2.71 (t, J = 6.0 Hz, 4 H), 2.48 (t, J = 6.1 Hz, 4 H).

Preparation of [Cd₃(L)₂(BDC)₃]₂-16DMF (**MOF-1a**)

A mixture of L (13.0 mg, 0.05 mmol), H₂BDC (8.3 mg, 0.05 mmol), Cd(ClO₄)₂·6H₂O (41.9 mg, 0.1 mmol), in DMF/CH₃OH (4 ml, v/v, 3:1) was sealed in a 20 ml glass vial and heated at 90 °C for 72 h, and then slowly cooled to room temperature. Light yellow block crystals of **MOF-1a** were isolated, washed with DMF and CH₃OH, and then dried in the air (yield about 50%). Anal. Calcd (%) for **MOF-1a** (C₁₅₂H₂₂₀N₃₆O₄₀Cd₆): C, 47.22; H, 5.74; N, 13.04; found: C, 47.12; H, 5.78; N, 13.56. IR (KBr, cm⁻¹, Figure S1a in the Supporting Information): 3406 (w), 3128 (m), 1659 (w), 1564 (s), 1503 (w), 1340 (s), 1105 (w), 1014 (w), 892 (w), 827 (m), 788 (s), 663 (w), 509 (m).

Preparation of [Cd₃(L)₂(BDC)₃]₂ (**MOF-1b**)

The acetone-exchanged **MOF-1a** was obtained by immersing the as-synthesized sample **MOF-1a** in acetone for 2 days to remove the non-volatile solvent molecules. The solvent was replaced by fresh acetone every 6 h. The colorless powder **MOF-1b** was obtained by drying acetone-exchanged **MOF-1a** under vacuum for 24 h at 40 °C. Removal of all solvent molecules was checked by TG. The structural data of **MOF-1b** were gotten by XRD. Anal. Calcd (%) for **MOF-1b** (C₁₀₄H₁₀₈N₂₀O₂₄Cd₆): C, 46.32; H, 4.04; N, 10.39; found: C, 46.52; H, 4.11; N, 10.51.

Preparation of Propargylamines

The substrates **1a-1f** were obtained from commercial suppliers and used as received without further purification. Substrates **1g** and **1h** were prepared according to the previously reported method.^[21]

Synthesis of Substrates 1i-1m ^[22]

To a 25 ml Schlenk flask equipped with a magnetic stir bar was charged with PdCl₂(PPh₃)₂ (56 mg, 0.08 mmol, 1 mol%), CuI (31 mg, 0.16 mmol, 2 mol%), idobenzene derivatives (8.0 mmol, 1.0 equiv), terminal propargylamine derivatives (8.0 mmol, 1.0 equiv) and NEt₃ (8 ml). The mixture was stirred at 60 °C under nitrogen atmosphere for 12 h. After cooling to room temperature, the mixture was diluted with ethyl acetate and the phases were separated. The crude product was further purified by column chromatography on silica gel (EtOAc/hexane = 1:5).

General Procedure for Carboxylative Cyclization of CO₂ with Propargylamines

To a 50 ml autoclave, propargylamines (1.0 mmol), indicated amount of the catalyst **MOF-1a** or **MOF-1b**, and acetonitrile (3 ml) were added. The air in the autoclave was replaced by CO₂ gas (the purity of the CO₂ is 99.999%). The autoclave was sealed and stirred at 60 °C for 24 h. After cooling to room temperature, the gas inside the autoclave was slowly released. The crude mixture was filtrated, and the filtration was concentrated. Pure product was obtained by silica gel column chromatography.

Acknowledgements

We gratefully acknowledge the National Natural Science Foundation of China (grant nos. 21331002, 21573106 and 21671097) and the National Basic Research Program of China (grant no. 2017YFA0303500) for financial support of this work. This work was also supported by a Project Funded by the Priority Academic Program Development of Jiangsu Higher Education Institutions.

Keywords: metal–organic framework • carboxylative cyclization • carbon dioxide • structural transformation • selective catalytic property

- [1] a) J. Hu, J. Ma, Q. Zhu, Z. Zhang, C. Wu, B. Han, *Angew. Chem. Int. Ed.* **2015**, *54*, 5399–5403; b) Y. L. Zhao, J. K. Qiu, L. Tian, Z. Y. Li, M. H. Fan, J. J. Wang, *ACS Sustainable Chem. Eng.* **2016**, *4*, 5553–5560; c) T. V. Nguyen, W. J. Yoo, S. Kobayashi, *Angew. Chem. Int. Ed.* **2015**, *54*, 9209–9212; d) X. Wang, M. Nakajima, R. Martin, *J. Am. Chem. Soc.* **2015**, *137*, 8924–8927; e) K. Fujita, A. Fujii, J. Sato, S.-y. Onozawa, H. Yasuda, *Tetrahedron Lett.* **2016**, *57*, 1282–1284; f) K. Fujita, J. Sato, H. Yasuda, *Synlett* **2015**, *26*, 1106–1110; g) R. Nicholls, S. Kaufhold, B. N. Nguyen, *Catal. Sci. Technol.* **2014**, *4*, 3458–3462; h) Z. Xin, C. Lescot, S. D. Friis, K. Daasbjerg, T. Skrydstrup, *Angew. Chem. Int. Ed.* **2015**, *54*, 6862–6866; i) M. S. Liu, L. Liang, X. Li, X. X. Gao, J. M. Sun, *Green Chem.* **2016**, *18*, 2851–2863; j) M. S. Liu, X. Y. Lu, L. Shi, F. X. Wang, J. M. Sun, *ChemSusChem* **2017**, *10*, 1110–1119; k) M. S. Liu, J. W. Lan, L. Liang, J. M. Sun, M. Arai, *J. Catal.* **2017**, *347*, 138–147; l) M. S. Liu, K. Q. Gao, L. Liang, J. M. Sun, L. Sheng, M. Arai, *Catal. Sci. Technol.* **2016**, *6*, 6406–6416.
- [2] a) N. Volz, J. Clayden, *Angew. Chem. Int. Ed.* **2011**, *50*, 12148–12155; b) T. Jiang, X. Ma, Y. Zhou, S. Liang, J. Zhang, B. Han, *Green Chem.* **2008**, *10*, 465–469.
- [3] a) A. Ueno, Y. Kayaki, T. Ikariya, *Green Chem.* **2013**, *15*, 425–430; b) D. B. Nale, S. Rana, K. Parida, B. M. Bhanage, *Appl. Catal., A* **2014**, *469*, 340–349; c) T. Y. Ma, S. Z. Qiao, *ACS Catal.* **2014**, *4*, 3847–3855; d) T. A. Mukhtar, G. D. Wright, *Chem. Rev.* **2005**, *105*, 529–542; e) C. Das Neves Gomes, O. Jacquet, C. Villiers, P. Thuéry, M. Ephritikhine, T. Cantat, *Angew. Chem. Int. Ed.* **2012**, *51*, 187–190.
- [4] a) S. Hase, Y. Kayaki, T. Ikariya, *ACS Catal.* **2015**, *5*, 5135–5140; b) K. Yamashita, S. Hase, Y. Kayaki, T. Ikariya, *Org. Lett.* **2015**, *17*, 2334–2337; c) G. Haufe, S. Suzuki, H. Yasui, C. Terada, T. Kitayama, M. Shiro, N. Shibata, *Angew. Chem. Int. Ed.* **2012**, *51*, 12275–12279; d) Q. W. Song, Z. H. Zhou, H. Yin, L. N. He, *ChemSusChem* **2015**, *8*, 3967–3972; e) S. Hase, Y. Kayaki, T. Ikariya, *Tetrahedron Lett.* **2014**, *55*, 3013–3016; f) R. Yuan, Z. Lin, *ACS Catal.* **2015**, *5*, 2866–2872.
- [5] a) M. Wang, Q. Song, R. Ma, J. Xie, L. He, *Green Chem.* **2016**, *18*, 282–287; b) D. Zhao, X. H. Liu, Z. Z. Shi, C. D. Zhu, Y. Zhao, P. Wang, W. Y. Sun, *Dalton Trans.* **2016**, *45*, 14184–14190; c) L. Y. Kong, Z. H. Zhang, H. F. Zhu, H. Kawaguchi, T. Okamura, M. Doi, Q. Chu, W. Y. Sun, N. Ueyama, *Angew. Chem. Int. Ed.* **2005**, *44*, 4352–4355; d) S. Yuan, L. F. Zou, H. X. Li, Y. P. Chen, J. S. Qin, Q. Zhang, W. G. Lu, M. B. Hall, H. C. Zhou, *Angew. Chem. Int. Ed.* **2016**, *55*, 10776–10780; e) A. Corma, H. García, F. X. Llabrés i Xamena, *Chem. Rev.* **2010**, *110*, 4606–4655; f) Y. L. Li, D. Zhao, Y. Zhao, P. Wang, H. W. Wang, W. Y. Sun, *Dalton Trans.* **2016**, *45*, 8816–8823; g) J. Y. Hu, J. Ma, Q. G. Zhu, Z. F. Zhang, C. Y. Wu, B. X. Han, *Angew. Chem. Int. Ed.* **2015**, *54*, 5399–5403; h) H. H. Wang, L. Hou, Y. Z. Li, C. Y. Jiang, Y. Y. Wang, Z. G. Zhu, *ACS Appl. Mater. Interfaces* **2017**, *9*, 17969–17976; i) O. V. Zalomaeva, A. M. Chibiryayev, K. A. Kovalenko, O. A. Kholdeeva, B. S. Balzhinimaev, V. P. Fedin, *J. Catal.* **2013**, *298*, 179–185; j) C. Martín, G. Fiorani, A. W. Kleij, *ACS Catal.* **2015**, *5*, 1353–1370; k) S. Yuan, L. F. Zou, H. X. Li, Y. P. Chen, J. S. Qin, Q. Zhang, W. G. Lu, M. B. Hall, H. C. Zhou, *Angew. Chem. Int. Ed.* **2016**, *55*, 10776–10780; l) P. Z. Li, X. J. Wang, J. Liu, J. S. Lim, R. Zou, Y. Zhao, *J. Am. Chem. Soc.* **2016**, *138*, 2142–2145; m) H. H. Wang, L. Hou, Y. Z. Li, C. Y. Jiang, Y. Y. Wang, Z. G. Zhu, *ACS Appl. Mater. Interfaces* **2017**, *9*, 17969–17976; n) C. Y. Gao, H. R. Tian, J. Ai, L. J. Li, S. Dang, Y. Q. Lan, Z. M. Sun, *Chem. Commun.* **2016**, *52*, 11147–11150.
- [6] a) L. Kovbasyuk, R. Krämer, *Chem. Rev.* **2004**, *104*, 3161–3188; b) V. Blanco, D. A. Leigh, V. Marcos, *Chem. Soc. Rev.* **2015**, *44*, 5341–5370.
- [7] a) S. Hasegawa, S. Horike, R. Matsuda, S. Furukawa, K. Mochizuki, Y. Kinoshita, S. Kitagawa, *J. Am. Chem. Soc.* **2007**, *129*, 2607–2614; b) T. M. McDonald, J. A. Mason, X. Q. Kong, E. D. Bloch, D. Gygi, A. Dani, V. Crocellà, F. Giordano, S. O. Odoh, W. S. Drisdell, B. Vlaisavljevich, A. L. Dzubak, R. Poloni, S. K. Schnell, N. Planas, K. Lee, T. Pascal, L. F. Wan, D. Prendergast, J. B. Neaton, B. Smit, J. B. Kortright, L. Gagliardi, S. Bordiga, J. A. Reimer, J. R. Long, *Nature* **2015**, *519*, 303–308; c) H. Li, K. C. Wang, D. W. Feng, Y. P. Chen, W. Verdegaal, H. C. Zhou, *ChemSusChem* **2016**, *9*, 2832–2840; d) L. Sarkisov, R. L. Martin, M. Haranczyk, B. Smit, *J. Am. Chem. Soc.* **2014**, *136*, 2228–2231.
- [8] a) A. Schneemann, V. Bon, I. Schwedler, I. Senkovska, S. Kaskel, R. A. Fischer, *Chem. Soc. Rev.* **2014**, *43*, 6062–6096; b) J. P. S. Mowat, V. R. Seymour, J. M. Griffin, S. P. Thompson, A. M. Z. Slawin, D. Fairen-Jimenez, T. Dueren, S. E. Ashbrook, P. A. Wright, *Dalton Trans.* **2012**, *41*, 3937–3941; c) C. Mellot-Draznieks, C. Serre, S. Surble, N. Audebrand, G. Férey, *J. Am. Chem. Soc.* **2005**, *127*, 16273–16278; d) S. Bureekaew, H. Sato, R. Matsuda, Y. Kubota, R. Hirose, J. Kim, K. Kato, M. Takata, S. Kitagawa, *Angew. Chem. Int. Ed.* **2010**, *49*, 7660–7664; e) O. K. Farha, I. Eryazici, N. C. Jeong, B. G. Hauser, C. E. Wilmer, A. A. Sarjeant, R. Q. Snurr, S. T. Nguyen, A. O. Yazaydin, J. T. Hupp, *J. Am. Chem. Soc.* **2012**, *134*, 15016–15021.
- [9] M. H. Beyzavi, C. J. Stephenson, Y. Y. Liu, O. Karagiari, J. T. Hupp, O. K. Farha, *Frontiers in Energy Research, section Carbon Capture, Storage, and Utilization*, **2015**, *2*.
- [10] a) J. Seo, R. Matsuda, H. Sakamoto, C. Bonneau, S. Kitagawa, *J. Am. Chem. Soc.* **2009**, *131*, 12792–12800; b) Y. W. Ren, Y. C. Shi, J. X. Chen, S. R. Yang, C. R. Qi, H. F. Jiang, *RSC Advances* **2013**, *3*, 2167–2170.
- [11] a) R. Nicholls, S. Kaufhold, B. N. Nguyen, *Catal. Sci. Technol.* **2014**, *4*, 3458–3462; b) N. D. Ca, B. Gabriele, G. Ruffolo, L. Veltri, T. Zanetta, M. Costa, *Adv. Synth. Catal.* **2011**, *353*, 133–146; c) Y. P. Ren, J. J. Shim, *ChemCatChem* **2013**, *5*, 1344–146.
- [12] V. A. Blatov, TOPOS, A Multipurpose Crystallochemical Analysis with the Program Package, Samara State University, Russia, **2009**.
- [13] A. L. Spek, PLATON, A Multipurpose Crystallographic Tool, Utrecht University, Utrecht, The Netherlands, **2001**.
- [14] a) A. A. Coelho, *J. Appl. Crystallogr.* **2005**, *38*, 455–461; b) C. Guguta, H. Meeke, R. de Gelder, *Cryst. Growth Des.* **2006**, *6*, 2686–2692.
- [15] a) P. P. Cui, Y. Zhao, G. C. Lv, Q. Liu, X. L. Zhao, Y. Lu, Sun, W. Y. *CrystEngComm* **2014**, *16*, 6300–6308; b) P. Llewellyn, S. Bourrelly, C. Serre, Y. Filinchuk, G. Férey, *Angew. Chem. Int. Ed.* **2006**, *45*, 7751–7754; c) L. J. Chen, J. P. S. Mowat, D. Fairen-Jimenez, C. A. Morrison, S. P. Thompson, P. A. Wright, T. Düren, *J. Am. Chem. Soc.* **2013**, *135*, 15763–15773; d) J. P. Zhang, S. K. Ghosh, J. B. Lin, S. Kitagawa, *Inorg Chem.* **2009**, *48*, 7970–7976.
- [16] a) K. Kamata, T. Kimura, H. Sunaba, N. Mizuno, *Catalysis Today* **2014**, *226*, 160–166; b) Y. Kayaki, M. Yamamoto, T. Ikariya, *Angew. Chem. Int. Ed.* **2009**, *48*, 4194–4197; c) Y. Kayaki, M. Yamamoto, T. Ikariya, *J. Org. Chem.* **2007**, *72*, 647–649; d) Y. Gu, F. Shi, Y. Deng, *J. Org. Chem.* **2004**, *69*, 391–394; e) H. F. Jiang, A. Z. Wang, H. L. Liu, C. R. Qi, *Eur. J. Org. Chem.* **2008**, 2309–2312; f) N. D. Ca, B. Gabriele, G. Ruffolo, L. Veltri, T. Zanetta, M. Costa, *Adv. Synth. Catal.* **2011**, *353*, 133–146; g) M. Yoon, R. Srirambalaji, K. Kim, *Chem. Rev.* **2012**, *112*, 1196–1231.
- [17] S. C. McKellar, S. A. Moggach, *Acta Cryst.* **2015**, *B71*, 587–607.

- [18] a) A. Dhakshinamoorthy, M. Alvaro, H. Garcia, *Chem. Commun.* **2012**, 48, 11275–11288; b) L. C. Li, R. Matsuda, I. Tanaka, H. Sato, P. Kanoo, H. J. Jeon, M. L. Foo, A. Wakamiya, Y. Murata, S. Kitagawa, *J. Am. Chem. Soc.* **2014**, 136, 7543–7546.
- [19] a) C. Miranda, F. Escartí, L. Lamarque, M. J. R. Yunta, P. Navarro, E. García-España, M. L. Jimeno, *J. Am. Chem. Soc.* **2004**, 126, 823–833; b) M. M. Abdel-Atty, N. A. Farag, S. E. Kassab, R. A. T. Serya, K. A. M. Abouzid, *Bioorg. Chem.* **2014**, 57, 65–82.
- [20] a) G. M. Sheldrick, *Acta Crystallogr. Sect. A: Found. Crystallogr.* **2008**, 64, 112–122; b) G. M. Sheldrick, SHELXL-2014, Program for crystal structure refinement, University of Göttingen, Göttingen, Germany, **2014**.
- [21] B. M. Trost, M. T. Rudd, *J. Am. Chem. Soc.* **2005**, 127, 4763–4776.
- [22] S. Hase, Y. Kayaki, T. Ikariya, *Organomet* **2013**, 32, 5285–5288.

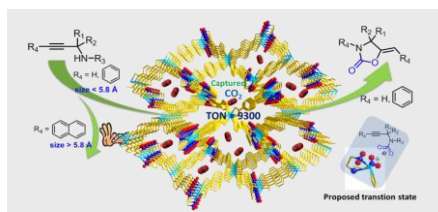
WILEY-VCH

Accepted Manuscript

Entry for the Table of Contents (Please choose one layout)

Layout 2:

FULL PAPER



This work describes the construction of a flexible and switchable 3D **MOF-1a** which is decorated with NH_2 -groups not only can realize the capture of CO_2 but also demonstrates its selective heterogeneous catalytic property, which depends on the size of the catalytic substrates, like an imitation of sophisticated biological systems.

Dan Zhao, Xiao-Hui Liu, Chendan Zhu,
Yan-Shang Kang, Peng Wang,
Zhuangzhi Shi, Yi Lu,* and Wei-Yin Sun*

Page No. – Page No.

**Efficient and Reusable Metal–Organic
Framework Catalyst for Carboxylative
Cyclization of Propargylamines with
Carbon Dioxide**